J Mater Sci (2008) 43:7338–7343
DOI 10.1007/s10853-008-2875-8

ULTRAFINE-GRAINED MATERIALS

Irradiation behavior of nanostructured 316 austenitic stainless steel

B. Radiguet · A. Etienne · P. Pareige · X. Sauvage · R. Valiev

Received: 9 March 2008 / Accepted: 10 July 2008 / Published online: 7 August 2008

Abstract In order to get information about radiation resistance of ultrafine grained austenitic stainless steels, a 316 steel was deformed by high pressure torsion. The mean diameter of the grain after deformation was 40 nm. This material was annealed at 350 °C for 24 h or irradiated with 160 keV iron ions at 350 °C. Changes in the microstructure during annealing or irradiation were characterised by transmission electron microscopy (grain size) and laser assisted tomographic atom probe (solute distribution). Results indicate that this annealing has no influence on the grain size whereas the grain diameter increases under irradiation. Concerning the solute distribution, atom probe investigations show evidence of radiation-induced segregation at grain boundaries. Indeed, after irradiation, grain boundaries are enriched in nickel and silicon and depleted in chromium. On the contrary, no intragranular extended defects or precipitation are observed after irradiation.

Introduction

Internal structures of pressurized water reactor (PWR), which maintain the fuel assemblies, are made of austenitic stainless steels (ASS). Due to the close vicinity of these structures with reactor core, they are submitted to neutron irradiation at high doses (up to 100 displacements per atom (dpa) at the PWR end of life). Neutron irradiation has a detrimental effect on the macroscopic properties of ASS. Indeed, under irradiation, hardening [1, 2] and loss of corrosion resistance [3] are observed. This evolution can result in the cracking of the bolt of the internal structure by irradiation assisted stress corrosion cracking (IASSC) [4–6].

The degradation of the macroscopic properties of ASS is strongly correlated with the evolution of their microstructure. Inside grains, different features are formed under neutron irradiation: interstitial dislocation loops (Frank loops) [7], voids [8, 9], precipitates or solute clusters (NiSi [10, 11], γ' phase Ni_3Si [12, 13] and carbides [14, 15]). Moreover, the chemical composition of grain boundaries is modified during irradiation. Chromium depletion and, nickel and silicon enrichments are observed [4–6, 16]. The common point between all these transformations is that they are all due to the super-saturation of point defects (interstitial atoms and vacancies). On the one hand, point defects can agglomerate in the form of loops or voids. On the other hand, they can enhance solute atom diffusion, resulting in enhanced precipitation, or drag solute (inverse Kirkendall effect), resulting in radiation induced segregation (RIS) or precipitation (RIP) at point defect sinks.

Even if the microstructural origin of IASSC is not clearly identified, several authors have shown that each feature described previously, considered separately, is not able to lead to IASCC [17, 18]. Only the combination of these microstructural changes results in IASCC. Thus, ultrafine grained (UFG) materials are expected to have an increased IASCC resistance. Indeed, grain boundaries act as a sink for point defects. Since the volume fraction of grain boundaries increases as the size of grain decreases, a

B. Radiguet (✉) · A. Etienne · P. Pareige · X. Sauvage
Université de Rouen, Groupe de Physique des Matériaux, UMR CNRS 6634, ERT No. 1000 Avenue de l'Université BP 12, 76801 Saint Etienne du Rouvray, France
e-mail: Bertrand.radiguet@univ-rouen.fr

R. Valiev
Institute of Physics of Advanced Materials, Ufa State Aviation Technical University, 12K. Marx Street, 450000 Ufa, Russian Federation

large part of the point defects created by irradiation should annihilate [19–21], reducing radiation damage dramatically, especially intragranular damage. Moreover, the number of point defects annihilating per unit of surface of the grain boundary is expected to be smaller when the volume fraction of grain boundaries increases. Therefore, intergranular RIS could be less intense in UFG materials.

In order to get information about the radiation behaviour of UFG ASS, a cold-worked (CW) ASS type 316 used in internal structures of French PWR was nanostructured by high pressure torsion (HPT). The microstructure of this material was characterised by X-ray diffraction (XRD), transmission electron microscopy (TEM) and laser assisted tomographic atom probe (LATAP) in the as-deformed state, after iron ion irradiation at 350 °C (∼temperature of internal structures in PWR) up to 10 dpa, and also after annealing treatment at 350 °C in order to separate temperature and irradiation effects.

Experimental procedure is described in the following part. Results are described and discussed afterwards.

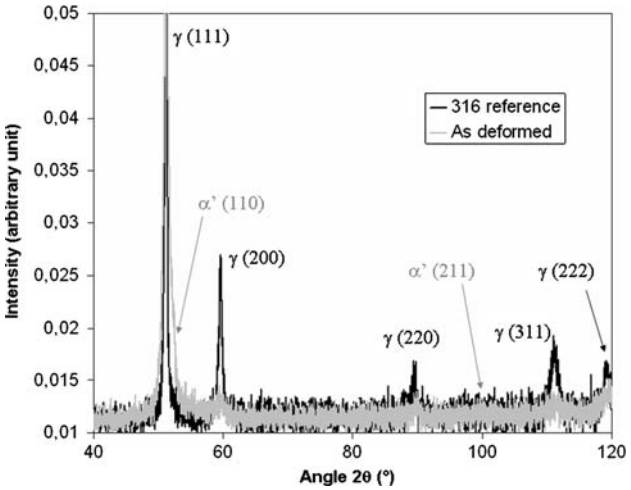

Fig. 1 X-ray diffraction spectra obtained on a CW 316 ASS before (black) and after (grey) deformation at room temperature by high pressure torsion under 5 GPa. Peaks characteristic of austenite are visible on both spectra. After deformation, peaks are enlarged and small peaks characteristic of α' martensite appear

Experimental

The initial material is a cold-worked (CW) 316 ASS which bolts maintaining internal structures in French PWR are made of. The bulk composition of this steel is given in the Table 1. Its initial grain size is about 40 μm. It was prepared under the shape of plates of 20-mm diameter and 0.5-mm thickness. Four plates were deformed at room temperature by HPT under a 5 GPa hydrostatic pressure [22] at the Institute of Physics of Advanced Materials in Ufa. Number of turns was equal to five, which corresponds to a strain shear of about 625 at the periphery of the plates. XRD spectra obtained from initial and as-deformed steels are depicted in Fig. 1. Comparison between the two spectra indicates that the steel stays mainly austenitic after deformation although a very slight amount of α' martensite appears. Such transformation ($\gamma \rightarrow \alpha'$) has been already observed and studied during the deformation of ASS [23, 24] and is not discussed here.

After deformation one plate was annealed at 350 °C during 24 h in argon atmosphere followed by air quench. After that, rods of 10-mm length and 0.3 × 0.3-mm^2 section, and disks of 3-mm diameter were cut from the periphery of each plate in order to prepare atom probe and TEM samples, respectively. Atom probe samples (tip with an end radius smaller than 50 nm) were obtained by electropolishing of the rod at about 10 V in a solution of 98% butoxyethanol and 2% perchloric acid. Thin foils were obtained by mechanical thinning of the disks down to 100 μm, followed by electropolishing in a solution of 70% of ethanol, 20% of 2-butoxyethanol and 10% perchloric acid. The operating temperature and voltage were 5 °C and 30 V, respectively.

Already prepared samples from as-deformed materials were irradiated with 160 keV Fe^+ ions. The depth of implantation of iron ions with this energy is around 50 nm, that is, the centre of an atom probe needle or of a TEM thin foil. TEM samples were irradiated in the ion implantor IRMA at the Centre de Spectrométrie Nucléaire et de

Table 1 Nominal composition of CW 316 SS and composition of UFG 316 SS after deformation at room temperature by high pressure torsion under 5 GPa and after irradiation at 350 °C to 10 dpa

	C	P	Si	Cr	Ni	Mn	Co	Mo	Cu
Nominal	0.25	0.048	1.34	17.7	10.02	1.13	0.11	1.3	0.21
UFG as-deformed	0.14	0.03	1.51	18.22	9.32	1.29	0.18	0.72	0.11
	0.01	*0.01*	*0.02*	*0.08*	*0.06*	*0.02*	*0.01*	*0.02*	*0.01*
UFG irradiated	0.25	0.04	1.42	17.58	11.45	1.32	0.02	1.27	0.14
	0.01	*0.01*	*0.02*	*0.07*	*0.05*	*0.02*	*0.01*	*0.02*	*0.01*

Some vanadium (not reported here) was also detected during atom probe analysis. Concentrations are given in at %. Balance is Fe. Numbers in italic are the uncertainties given by the standard deviation

Spectrométrie de Masse (CSNSM-Orsay-France) up to a dose of 2.6×10^{19} m^{-2}. Atom probe samples were irradiated in a similar implantor located at the Laboratoire de Physique de Matériaux (PHYMAT-Poitiers-France) up to 5.2×10^{19} m^{-2}. Using SRIM 2006 (http://www.srim.org/) [25] and the Kinchin Pease approximation [26], these doses correspond to 5 and 10 dpa, respectively. Both irradiations were performed at 350 °C, which is the irradiation temperature of internal structures in a PWR.

As-deformed, annealed and irradiated samples were characterised by TEM at the Department of Materials of Oxford University using a Phillips CM20. As-deformed and irradiated samples were also characterised with the LATAP developed at the Groupe de Physique des Matériaux [27, 28]. Results are described and discussed in the following part.

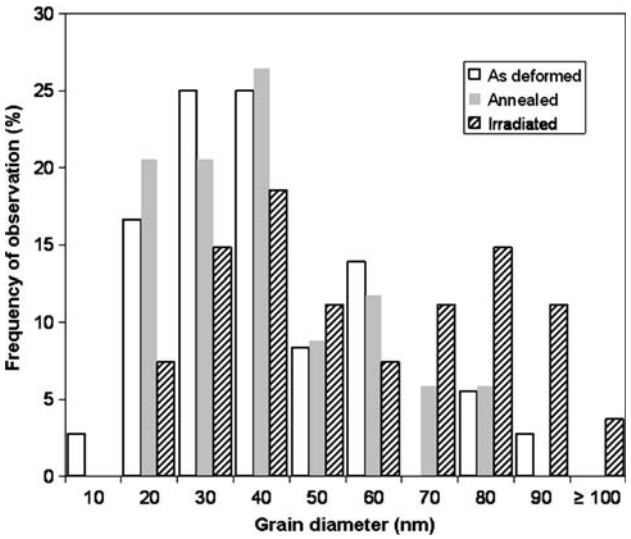

Fig. 3 Size distribution of grains in UFG 316 ASS after (a) deformation at room temperature by high pressure torsion under 5 GPa, (b) annealing at 350 °C for 24 h and (c) irradiation at 350 °C to 5 dpa

Results and discussion

Grain size

Samples irradiated up to 5 dpa were characterised by TEM. Dark field images and corresponding diffraction patterns of the as-deformed, annealed and irradiated samples are represented in Fig. 2. As far as diffraction patterns are concerned, in the two unirradiated samples, they are continuous rings. In the irradiated samples, rings are spottier. This indicates that in the as-deformed samples as well as the annealed samples, lot of grains with random crystallographic orientations are diffracting. After irradiation, grains still have random orientations, but there is less diffracting grains. The ratios between the radii of the rings are the same in all samples. They correspond to austenite atomic plane reflections. Moreover, two rings with a weak intensity are detected. They correspond to (110) and (220) reflections of α' martensite. Evidence of a small amount of martensite is in good agreement with XRD results.

Dark field images depicted in Fig. 2 were obtained from (111) and (200) reflections of austenite and (110) planes of martensite. The grain size distributions for each sample were determined using such pictures. For each sample, at least 30 grains were measured. The results are reported in Fig. 3. It appears that annealing at 350 °C for 24 h has no effect on the grain size. Indeed, the mean grain diameter is about 40 nm in both as-deformed and annealed materials. These results agree well with previous observation of Belyakov et al. [29]. These authors studied the effect of isothermal annealing on a 304 ASS with strain-induced sub-micron grains (~300 nm in diameter). They did not observe recrystallisation after annealing during 450 s if the temperature is below 1,000 K (i.e. below the recrystallisation temperature of ASS). In our case the temperature is largely below this limit, and therefore, recrystallisation can not occur.

Results are different after irradiation. As seen in Fig. 3, the proportion of small grains decreases, whereas grains bigger than 100 nm appear. The mean grain diameter is then about 60 nm. Such behaviour was already observed by Rose et al. [30] in irradiated palladium. Taking into

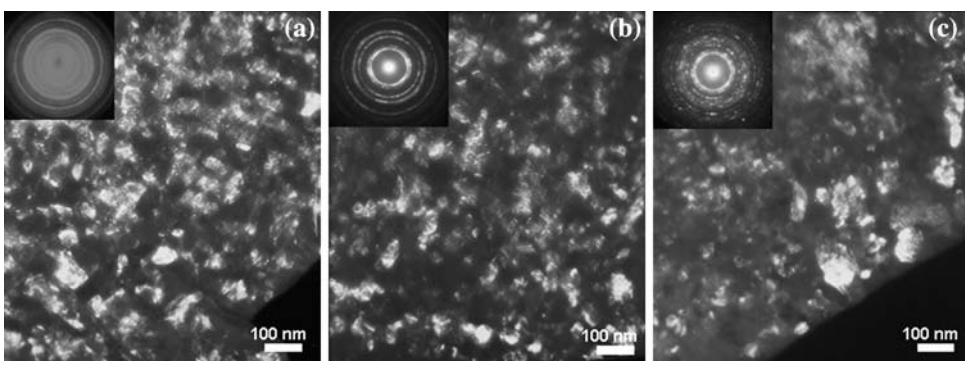

Fig. 2 Dark field images of UFG 316 ASS after (**a**) deformation at room temperature by high pressure torsion under 5 GPa, (**b**) annealing at 350 °C for 24 h and (**c**) irradiation at 350 °C to 5 dpa. Corresponding diffraction patterns are also represented

account the results obtained on annealed samples, the grain growth can not be attributed to annealing effect. Using molecular dynamic simulations, Voegeli et al. [21] suggest that grain growth can occur during irradiation, if the volume of the displacement cascade created by the impact of an incident particle with an atom from the material overlaps a grain boundary. In this case, during cooling and shrinking of the cascade, recrystallisation occurs, resulting in the growth of the grain. If several displacement cascades overlap the same grain boundary, the growth of the grain is accumulated. In our irradiation conditions (1.4×10^{15} ions m^{-2} s^{-1} during 5 h), many cascade overlapping occur. Therefore, this mechanism could explain the observed grain growth in these nanostructured materials.

Solute distribution

Only the as-deformed and irradiated (10 dpa) samples were analysed by LATAP. The mean chemical composition measured for each kind of sample is reported in the Table 1. No significant variations of composition were observed in any material.

The total length of the matter analysed in the as-deformed material is about 600 nm. Since the mean diameter of a grain is about 40 nm, more than 10 grain boundaries should have been intercepted during these analyses. However, the 3D reconstruction and solute distribution do not show any evidence of the presence of grain boundaries in these volumes. On the contrary, solute atoms are homogeneously distributed in the material. This means that grain boundaries have the same chemical composition as the grains. This point can be explained by the fact that plastic deformation occurred at room temperature. This low temperature does not allow any mobility of atoms and grain boundaries cannot reach equilibrium composition.

In the irradiated material, nickel and silicon segregations are observed (Fig. 4). These segregations are plate shaped. They measure 2 nm in thickness. Such solute enrichments can only be attributed to segregations at grain boundaries. A concentration profile through one grain boundary (Fig. 5) shows that it is enriched in nickel up to 17 at.% and in silicon up to 4 at.%. It is also depleted in chromium ($\sim$13 at.%) and in molybdenum (not shown in Fig. 5). These values correspond to those given in literature for ASS irradiated at similar temperatures and doses [13, 31]. Thus, it appears that RIS also occurs in UFG 316 steels. Even if the composition of segregated grain boundaries observed here is similar to the values given in literature for irradiated 316 ASS, it is difficult to say if UFG steel has a beneficial effect on the intergranular RIS or not. Indeed, it must be kept in mind that the irradiation conditions are not exactly the same in this work (Fe^{+} irradiations) as what can be found in literature (neutrons or protons irradiations).

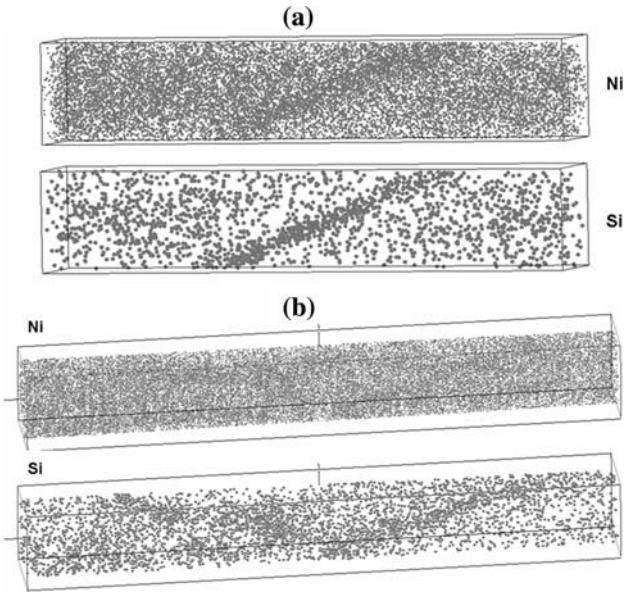

Fig. 4 3D reconstruction of two small volumes [(**a**) $10 \times 10 \times 50$ nm^3 and (**b**) $10 \times 10 \times 80$ nm^3] of UFG 316 ASS irradiated at 350 °C to 10 dpa. Only nickel and silicon are represented. Segregation of these solute atoms at grain boundaries appears clearly

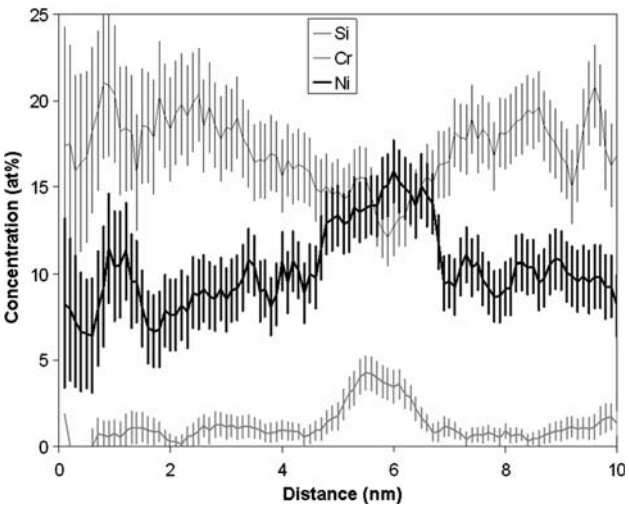

Fig. 5 Concentration profile through the grain boundary shown in Fig. 4a. In addition to Ni and Si enrichment, Cr depletion is observed

Thus, it is possible that the number of mobile point defects created here, and consequently, the flux of point defects towards grain boundaries are not the same as that under irradiations with others particles.

As far as intragranular distribution of the solutes is concerned, no solute enrichment or depletion was observed inside grains (Fig. 6). Indeed, solute atoms are homogeneously distributed inside grains after irradiation. This suggests that intragranular radiation damage is suppressed in UFG steel. In order to confirm this point, and in particular, to exclude any effect of the surface (atom probe

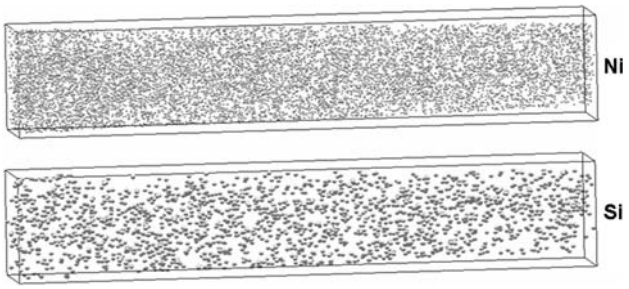

Fig. 6 3D reconstruction of a small volume ($10 \times 10 \times 50$ nm^3) of UFG 316 ASS irradiated at 350 °C to 10 dpa. This volume is located inside a grain (no grain boundary intercepted). Only nickel and silicon are represented. These solutes are homogeneously distributed

needles were irradiated), which also act as a sink for point defects elimination, results can be compared with those presented in [32]. It is shown in this paper that in atom probe needles of CW 316 ASS, irradiated at 350 °C with 160 keV iron ions up to 5 dpa, Si and Ni enriched clusters are formed. This clearly demonstrates that the tip surface does not suppress intragranular solute clustering. Since such clusters are not observed in nanostructured materials and since the only difference is the grain size (40 μm in CW 316 ASS and 40 nm here), it can be concluded that the decrease in the grain diameter limits dramatically the intragranular solute clustering. Moreover, some authors suggest that Ni and Si clustering is due to RIS on Frank loops [12, 13, 33]. Missing of Ni and Si clustering here may be an indication that there is no Frank loops formed in UFG steel. The reason could be the annihilation of interstitial atoms at the grain boundaries.

Conclusion

The behaviour under iron ion irradiation at 350 °C of UFG 316 ASS obtained by HPT was investigated by TEM and LATAP. It appears that,

1. The size of the grain increases during irradiation. Comparison between annealed and irradiated samples clearly demonstrates that growth is not due to temperature but irradiation damage.
2. Intergranular RIS occurs in UFG material with the same intensity as that in proton or neutron irradiated ASS.
3. However, no intragranular precipitation or segregation was observed. This point can be explained by annihilation of point defects at grain boundaries.

Since IASSC is a complex phenomenon between intragranular evolution and intergranular RIS, it can be assumed that the suppression of one component could suppress or at least limit IASCC in UFG 316 ASS. For this reason, UFG may have promising behaviour in PWR. Irradiations at higher doses and modelisation of the phenomenon are in progress.

Acknowledgements The authors gratefully thank EDF for providing 316 materials. Many thanks to Odile Kaïtasov (CSNSM-Orsay) and Michel Drouet (PHYMAT-Poitiers) for performing iron ion irradiations. The authors would like to thank M. Jenkins (Oxford) for TEM characterisations. The TEM investigations were supported by the IP3 project of the 6th Framework Programme of the European Commission: ESTEEM-Contract number 026019.

References

1. Grosssbeck ML, Ehrlich K, Wassilew C (1990) J Nucl Mater 174:264. doi:10.1016/0022-3115(90)90240-N
2. Odette GR, Lucas GE (1991) J Nucl Mater 179–181:572. doi:10.1016/0022-3115(91)90152-W
3. Lucas GE (1993) J Nucl Mater 206:287. doi:10.1016/0022-3115(93)90129-M
4. Bruemmer SM, Charlot LA, Simonen EP (1992) Proceedings of 5th international symposium on environmental degradation of materials in nuclear power Systems Water Reactors La Grange Park IL, 1992, pp 821
5. Bruemmer SM, Edwards DJ, Gertsman VY, Simonen EP (2001) Mat Res Soc Symp, vol 650
6. Allen TR, Was GS (1998) Acta Mater 46–10:3679
7. Pokor C, Brechet Y, Dubuisson P, Massoud J-P, Barbu A (2004) J Nucl Mater 326:19. doi:10.1016/j.jnucmat.2003.11.007
8. Mazias PJ (1993) J Nucl Mater 205:118. doi:10.1016/0022-3115(93)90077-C
9. Zinkle SJ, Mazias PJ, Stoller RE (1993) J Nucl Mater 206:266. doi:10.1016/0022-3115(93)90128-L
10. Kenik EA, Hojou K (1992) J Nucl Mater 191–194:1331. doi:10.1016/0022-3115(92)90691-D
11. Etienne A, Radiguet B, Pareige P, Massoud J-P, Pokor C, J Nucl Mater (submitted)
12. Edwards DJ, Simonen EP, Bruemmer SM (2003) J Nucl Mater 317:13. doi:10.1016/S0022-3115(03)00002-3
13. Edwards DJ, Simonen EP, Garner FA, Greenwood LR, Oliver BM, Bruemmer SM (2003) J Nucl Mater 317:32. doi:10.1016/S0022-3115(03)00003-5
14. Hashimoto N, Wakai E, Robertson JP (1999) J Nucl Mater 273:95. doi:10.1016/S0022-3115(99)00009-4
15. Bond GM, Sencer BH, Garner FA, Hamilton ML, Allen TR, Porter DL (1999). In: Bruemmer SM, Ford P, Was G (eds) 9th International conference on environmental degradation of materials in nuclear systems–water reactors, The Minerals, Metals and Materials Society, Pennsylvania
16. Watanabe S, Satu J, Sakaguchi N, Takahashi H, Namba C (1996) J Nucl Mater 239:200. doi:10.1016/S0022-3115(96)00422-9
17. Busby JT, Was GS, Kenik EA (2002) J Nucl Mater 302:20. doi:10.1016/S0022-3115(02)00719-5
18. Fukuya K, Nakano M, Fujii K, Torimaru T (2004) J Nucl Sci Technol 41–45:594. doi:10.3327/jnst.41.594
19. Nita N, Schaeublin R, Victoria M (2004) J Nucl Mater 329–333:953. doi:10.1016/j.jnucmat.2004.04.058
20. Samaras M, Derlet PM, Swygenhoven HV, Victoria M (2002) Phys Rev Lett 88:12. doi:10.1103/PhysRevLett.88.125505
21. Voegeli W, Albe K, Hahn H (2003) Nucl Instrum Methods B 202:230. doi:10.1016/S0168-583X(02)01862-1
22. Valiev RZ, Islamgaliev RK, Alexandrov IV (2000) Prog Mater Sci 45:103

23. Nagy E, Mertinger V, Tranta F, Solyom J (2004) Mater Sci Eng A378:308
24. De AK, Murdock DC, Mataya MC, Speer JG, Matlock DK (2004) Scripta Mater 50:1445. doi:10.1016/j.scriptamat.2004.03.011
25. Ziegler JF, Biersack JP, Littmark U (1985) The stopping and range of ions in solids. Pergamon Press, New York
26. Kinchin GH, Pease RS (1955) Rep Prog Phys 18:1. doi:10.1088/0034-4885/18/1/301
27. Blavette D, Bostel A, Sarrau JM, Deconihout B, Menand A (1993) Nature 363:432
28. Gault B, Vurpillot F, Vella A, Gilbert M, Menand A, Blavette D et al (2006) Rev Sci Instrum 77:043705. doi:10.1063/1.2194089
29. Belyakov A, Sakai T, Miura M, Kaibyshev R, Tsuzaki K (2002) Acta Mater 50:1547. doi:10.1016/S1359-6454(02)00013-7
30. Rose M, Balogh AG, Hahn H (1997) Beam Interact Mater Atoms. Nuc Inst and Met in Phys Res, Section B 127–128:119
31. Asano K, Fukuya K, Nakata K, Kodoma M (1992). In: Cubicciotti D (ed) Proceedings of the 5th international symposium on environmental degradation of materials in nuclear power systems water reactors, Monterey, CA, American Nuclear Society, La Grange Park, IL, 1992, p 838
32. Pareige P, Etienne A, Radiguet B, J Nucl Mater (accepted)
33. Pokor C, Massoud J-P, Pareige P, Garnier J, Loisnard D, Dubuisson P et al (2005) 12th international conference on environmental degradation of materials in nuclear systems—water reactors, The Minerals, Metals and Materials Society, Salt Lake City